ORIGINAL PAPER - EXPLORATION GEOLOGY

CrossMark

A comprehensive analysis of the sedimentology, petrography, diagenesis and reservoir quality of sandstones from the Oligocene Xiaganchaigou (E₃) Formation in the Lengdong area, Qaidam Basin, China

Jie He[1,2] · Hua Wang[1,2] · Chengcheng Zhang[4] · Xiangrong Yang[1,2] · Yunfei Shangguan[1,2] · Rui Zhao[1,2] · Yin Gong[1,2] · Zhixiong Wu[3]

Abstract

The sandstone from the Oligocene Xiaganchaigou Formation (E₃) in the Lengdong area, Qaidam Basin, China, is extensively distributed and acts as an effective regional reservoir for hydrocarbon accumulation. Based on thin sections, scanning electron microscopy (SEM), X-ray diffraction (XRD) image analysis and cathodoluminescence (CL), a comprehensive analysis of the sedimentology, petrography, diagenesis and reservoir quality of the Oligocene sandstone reservoirs of the Xiaganchaigou (E₃) Formation in the Lengdong area, Qaidam Basin, are studied. The sandstones in the Lengdong area are classified as argillaceous sandstone, silty sandstone, fine sandstone, medium sandstone, pebbly sandstone, conglomeratic sandstone and conglomerate based on their grain sizes, degrees of sorting, and matrix contents. Five sedimentary facies were identified in the Xiaganchaigou Formation (E₃) of the Lengdong area, Qaidam Basin: distributary channel, interdistributary bay, mouth bar, central bar and distal sand sheet facies. Their major diagenetic processes include compaction, carbonate cementation and feldspar and calcite cement dissolution. The porosity and permeability values of the fine sandstone, conglomerate, and conglomeratic sandstone are the highest, followed by those of the medium sandstone and silty sandstone, and the argillaceous sandstone and pebbly sandstone have the lowest porosity and permeability values. The diagenetic sequence in the study area ranges from the eodiagenesis B stage to the mesodiagenetic A stage. Compaction has significantly reduced the primary porosity. Carbonate cements, mainly calcite cements, occlude pores by precipitating in intergranular and intragranular spaces. Dissolution largely contributes to increasing the secondary porosity. The well-sorted and relatively coarser-grained sandstones that formed in higher-energy sedimentary facies (distributary channel, mouth bar and central bar) have a better reservoir quality than the poorly sorted, clay-rich sandstones that formed in low-energy environments (interdistributary bay and distal sand sheet). Based on the comprehensive analysis of petrographic data, diagenesis and sedimentary facies, the reservoir in the Lengdong area is classified into three types: type A, type B and type C. Type A, located in the center of the study area, is the most favorable reservoir, while type C sandstone is the last to consider when looking for a good reservoir. This study can guide hydrocarbon exploration in the Lengdong area, as well as in northwestern China and similar areas throughout the world.

Keywords Diagenesis · Petrography · Sedimentary facies · Reservoir quality · Xiaganchaigou Formation · Oligocene · Lengdong area · Qaidam Basin

Introduction

The Lengdong area, which is located in the northwestern North Qaidam Basin, covers a large part of the Qaidam Basin, which is a prolific petroleum-bearing basin in northwestern China. It has produced good industrial oil flow in the shallow layers and has shown good gas potential in

✉ Hua Wang
   wanghua@cug.edu.cn

Extended author information available on the last page of the article

deep Jurassic and basement rocks (Jia et al. 2013). Over the past few years, considerable interest has been focused on the Lengdong area due to its petroleum potential. Several researchers have performed numerous significant studies of the regional geology, sedimentology, tectonic evolution, and petroleum prospect of individual parts of the basin and its adjoining areas (Tian et al. 2011; Cao et al. 2013; Luo et al. 2013; Fu et al. 2015; Jing et al. 2017). However, studies of the reservoir properties and sandstone reservoir diagenesis and their implications for the reservoir quality are scarce, except for that of Chen et al. (2015).

In this regard, a gap exists between understanding the reservoir properties and their controlling factors on the reservoir quality of the Lengdong area, Qaidam Basin. To help fill this gap, this study conducts a comprehensive analysis of the sedimentology, petrography, diagenesis and reservoir quality of the Oligocene sandstones in the Lengdong area, Qaidam Basin, China, to characterize the reservoir and describe how its sedimentology, petrography, and diagenesis influence the reservoir quality. In addition, the evaluating parameters of the reservoir quality are selected to classify the reservoir types in the study area and thus to predict favorable reservoirs for petroleum exploration. These results could have practical significance for the hydrocarbon exploration in basins in northwestern China and other similar areas around the world.

Geological setting

The Qaidam Basin, which is located in the northeastern Tibetan Plateau, is a rhombic Meso-Cenozoic intracontinental sedimentary basin that developed on the Qaidam block during the pre-Jurassic period (Yin et al. 2008; Pang et al. 2012; Fu et al. 2015). It is a negative tectonic unit confined by the Altun, Qilian and east Kunlun mountains (Ritts et al. 1999) (Fig. 1a). The Qaidam Basin experienced three stages of evolution: a rifting trough-ocean stage in the Sinian to Lower and Middle Devonian; the Paleotethys stage in the late Devonian to Triassic; and an intracontinental basin stage in the Meso-Cenozoic (Jolivet et al. 2001). In the Meso-Cenozoic stage, thick continental clastic rocks were deposited in the Qaidam Basin. Influenced by the Indosinian and Yanshan movements, the Qaidam Basin rifted in the Jurassic and Cretaceous. In the late Cretaceous, the Lenghu structural belt was subjected to uplift and erosion due to the activity of the Sichuan movement, and it thus lacks middle and upper Jurassic and Cretaceous strata. Then, in the Paleogene, the Qaidam Basin entered a depression–subsidence phase due to the compression from the Himalayan movement. In the Neogene, thrust folds and faults formed with the continuous compression caused by the Himalayan movement. The northern margin of the Qaidam Basin can be structurally divided into several subtectonic units, including the Qilian uplift to the west and the Altun uplift, Maxian uplift,
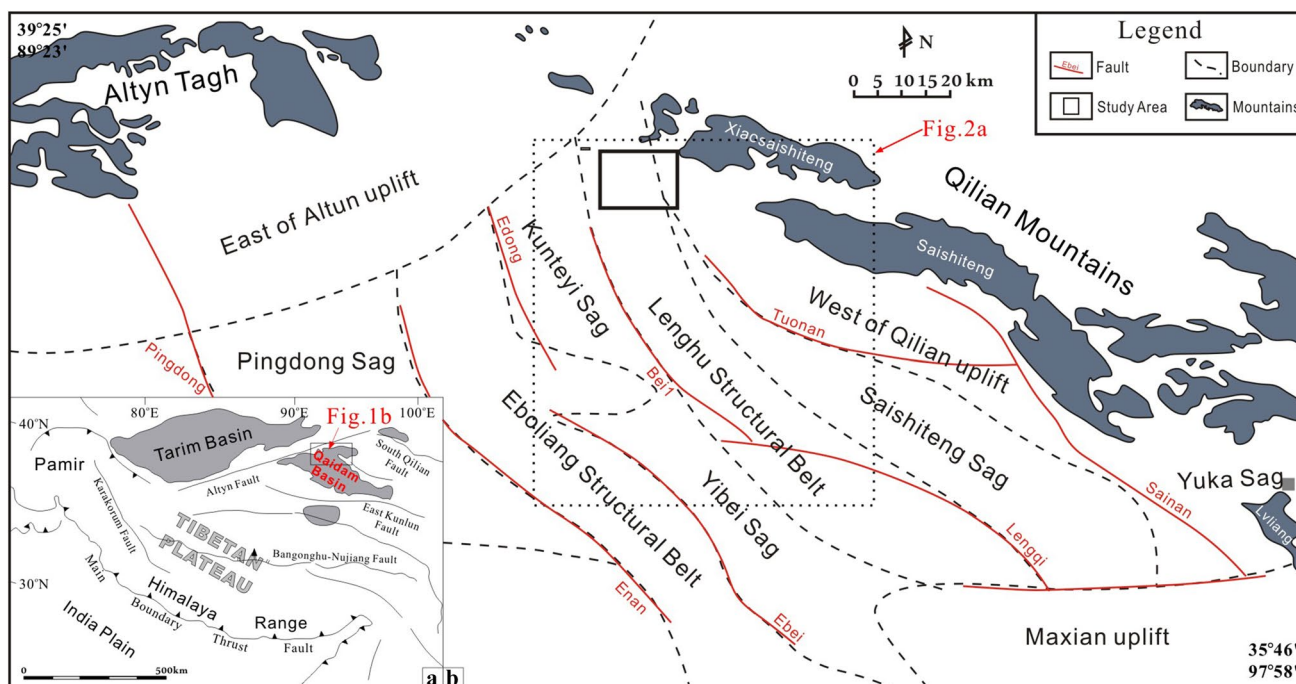

Fig. 1 **a** The regional geological setting and location of Qaidam Basin. The black rectangle indicates the study area shown in **b**. **b** Tectonic zones in the northern margin of Qaidam Basin (modified from Ref. Tian et al. 2018; Zhao et al. 2018)

Lenghu structural belt, Eboliang structural belt, Saishiteng Sag, Pingdong Sag, Kunteyi Sag and Yibei Sag to the east (Li et al. 2012; Chen et al. 2015) (Fig. 1b).

The Lengdong area is located to the north of the Lenghu structural belt (Fig. 2a). Uplift in the late Cretaceous resulted in the erosion or non-deposition of the Late Cretaceous and entire Jurassic strata in the Lengdong area. The Cenozoic sequences of the basin have been precisely constrained and defined by lithostratigraphic, magnetostratigraphic, seismic stratigraphic and palynologic data (Zhao et al. 2018). The Paleogene and Neogene stratigraphy in the Lengdong area can be divided into five formations, namely, from the base to the top, Lower Jurassic rock (J_1), the Paleocene and Eocene Lulehe Formation (E_{1+2}), the Oligocene Lower Xiaganchaigou Formation (E_3^1) and Upper Xiaganchaigou Formation (E_3^2), the Miocene Shangganchaigou Formation (N_1) and the Pliocene Xiayoushashan Formation (N_2^1) (Fig. 2b). The target formation of this study is the Xiaganchaigou (E_3) Formation, which is the major oil-bearing formation in this area. The Xiaganchaigou Formation (E_3) is extensively developed in the Lengdong area, with an average thickness of 300 meters. The Lower Xiaganchaigou Formation (E_3^1) consists of brownish-red sandstones intercalated with siltstones.

The Upper Xiaganchaigou Formation (E_3^2) comprises gray–green and gray sandstone interbedded with gray and dark gray mudstones (Tian et al. 2018).

The thermal history and burial history of the Lengdong area have been analyzed in detail using exploration and production well data synthesized with the Basinmod software by the Petro China Qinghai Oilfield Company (internal data). The current maximum burial depth of the Xiaganchaigou Formation in the Lengdong area, Qaidam Basin, is approximately 2500 m. The present-day geothermal gradient is 28.6 ± 4.6 °C/km, and the average surface temperature is approximately 10 °C (Li et al. 2016). The present-day maximum temperature at 2500 m is approximately 80 °C. Previous studies have shown that the organic carbon contents of the mudstone and shales in the Xiaganchaigou Formation range from 1.5 to 2.0%, and the organic matter is mainly type I and II kerogens. The source rocks are low mature to mature, with average vitrinite reflectance (Ro%) values ranging from 0.75 to 1.25% (Tian et al. 2018). The northeastern Lengdong area has become overpressured in the Lower Xiaganchaigou Formation (E_3^1), with formation pressure coefficients ranging from 1.2 to 1.8 (Tang 2016).
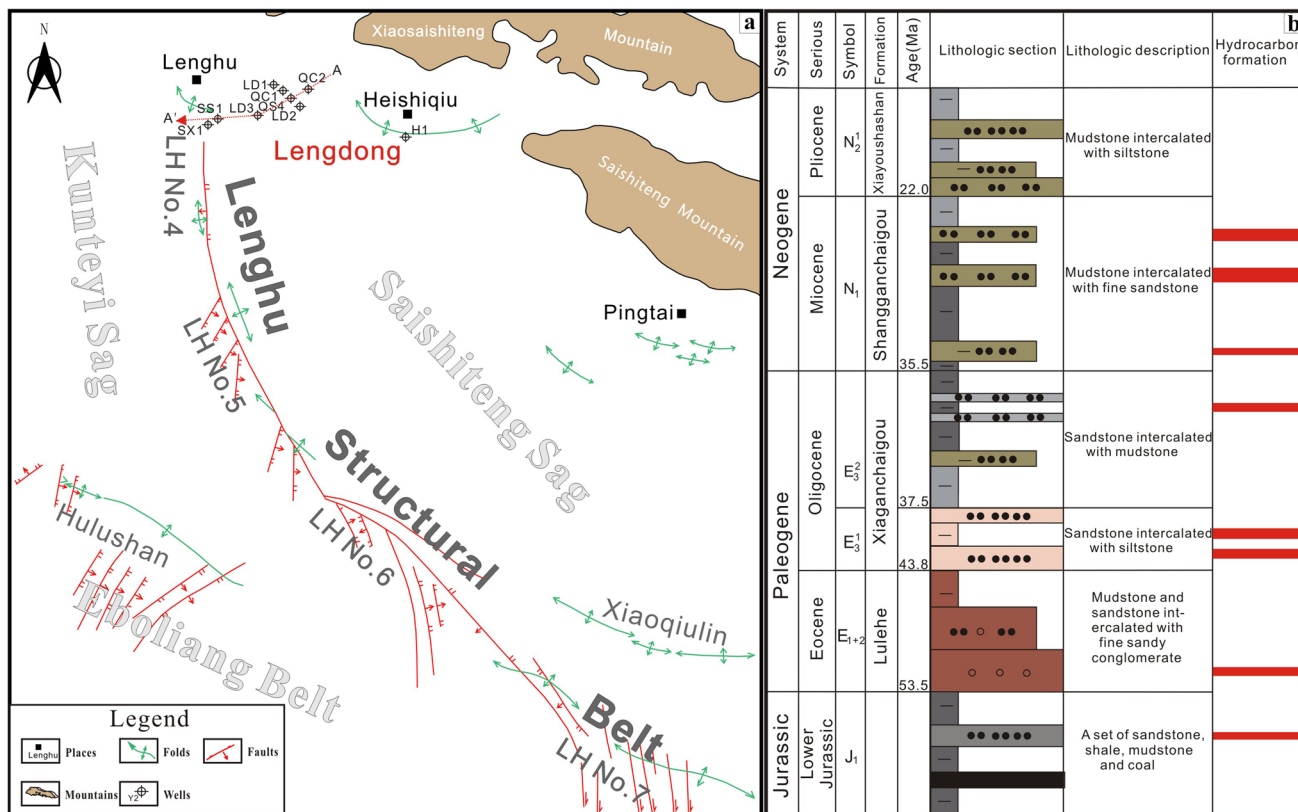

Fig. 2 **a** Structural location of Lenghu area and location of Lengdong in Lenghu area. **b** Stratigraphic divisions, lithology and hydrocarbon formations in Lengdong area. (modified from Ref. Tian et al. 2018; Zhao et al. 2018)

Materials and methods

Over 300 m of drilling cores from 15 wells and logging data [natural gamma (GR)] from 25 wells of the Xiaganchaigou Formation (E_3) in the Lengdong area, Qaidam Basin, were used to determine the sedimentary facies and indicate the distribution range of sedimentary facies. Rock composition data from 234 thin section samples and reservoir porosity and permeability data from 3225 samples were collected from the Petro China Qinghai Oilfield Company. The quantitative determination of porosity and permeability values was performed by an Ultrapore™ 300 Helium Pycnometer and porosimeter PASCAL 440 at the Exploration & Development Research Institute of the Petro China Qinghai Oilfield Company. In total, 50 thin sections were collected from 1149 to 1644 m in well SX1 in the Lengdong area. Fourteen samples were selected from 1184 to 1658 m in well SX1 in the Lengdong area for cathodoluminescence (CL) imaging. Thirty-eight thin sections from 1149 to 1645 m in Saixin1 were analyzed using scanning electron microscopy (SEM); 138 images were taken, along with four energy dispersive X-ray spectrometry (EDS) images.

Before thin sectioning, samples were vacuum processed with blue resin to reveal their porosity. Thin sections were stained with a mixed Alizarin Red-S and potassium ferricyanide solution to indicate carbonate minerals. All thin sections were analyzed for their rock mineralogy, diagenesis and visual porosity by optical microscopy. Point counting was performed on thin sections to determine their detrital grain contents and carbonate cements. Conventional counting (300 points) was used to analyze detrital compositions, including framework grains, cement, and porosity. Individual crystals (> 62.5 μm in diameter) were counted using a modified Gazzi–Dickinson method (Dickinson 1970; Zuffa 1980). The point counting distance was larger than the largest grain fraction, and the 2σ values for each individual mineral composition per thin section were calculated using the method of Van Der Plas and Tobi (1965).

Scanning electron microscopy (SEM) was performed with a JSM-5500LV SEM at the Petroleum Geology Analysis and Test Center, Research Institute of Exploration and Production of the Sinopec Zhongyuan Oilfield Company, China. The scanning electron microscope (SEM) is equipped with an SDD detector, pulse processor and workstation computer system with Esprit software. In addition, energy dispersive X-ray spectroscopy (EDS) was used for the qualitative identification of minerals. The thin sections were polished to thicknesses of 0.03–0.06 mm for cathodoluminescence (CL) analyses, which were carried out using a CITL Cold Cathode Luminescence 8200mk3, with an excitation energy of 20 kV and a beam current of 400 mA.

The sample treatment method used for X-ray diffraction (XRD) refers to those of Moore and Reynolds (1989) and Hillier and Hillier (2001). To improve the precision, the outer rim (approximately 5 mm) of each core was removed to avoid possible contamination from drilling mud. Afterwards, the sandstones were crushed to 2 mm pieces, disaggregated with diluted H_2O_2 and treated with a 400 W ultrasonic probe (2×3 min). The < 2 mm fractions were obtained by sedimentation. The samples containing carbonates were treated with a 0.1 M ethylene diamine tetraacetic acid (EDTA) solution (pH 4.5) and then washed with distilled water. The fractions were first air-dried and then treated with ethylene glycol and heated (I-300 °C, II-550 °C).

Smectite includes random-ordered mixed-layer illite/smectite (R_0: 10–50% illite), whereas ordered illite/smectite ($R_1 > 50\%$ illite) is represented as I/S. The quantities of smectite and I/S were determined based on the integrated area of the expanded 17 Å peak with the ethylene glycol treatment, whereas the type of ordering (R_0, R_1 or R_3) was determined based on the location of the smectite 003/illite 002 peak. Slow scans were completed for accurate feldspar determination (bulk: 26–28.5°2θ; 0.01°2θ/4 s) in addition to kaolinite/chlorite determination (clay AD: 24–26°2θ; 0.01°2θ/4 s).

Results

Petrography

Sandstone reservoir compositions

The grain sizes of the Oligocene sandstone reservoirs in the Lengdong area range from mud-sized to coarse-grained in size. The contents of the coarse, medium, fine, silty sand and mud fractions are summarized in Table 1. Fine- to coarse-grained sands are the main components of these sandstones (Fig. 3a). Based on their grain size compositions, the sandstones in the study area can be identified as argillaceous sandstone, silty sandstone, fine sandstone, medium

Table 1 Grain compositions and characteristics of Oligocene sandstone reservoirs in the Lengdong area

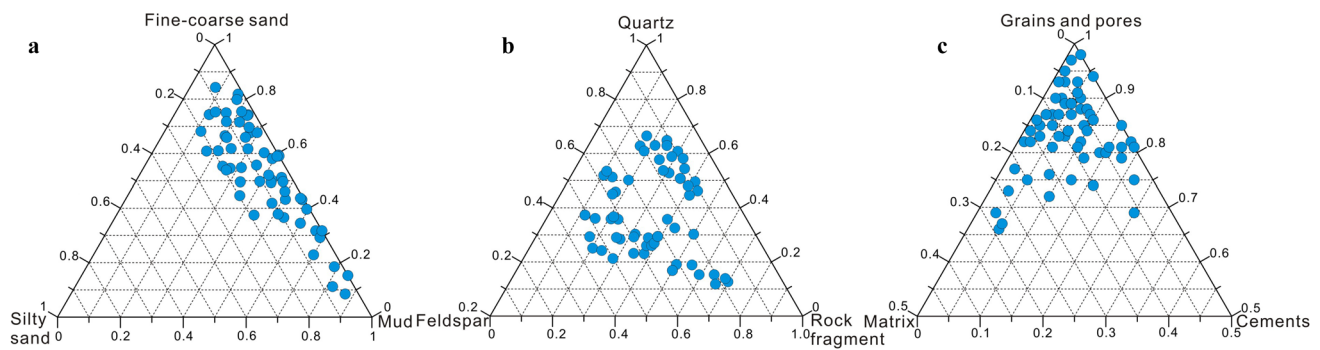| Grain grade	Min	Max	Avg
Coarse sand (%)	0	31.36	18.49
Medium sand (%)	0	57.71	25.26
Fine sand (%)	0	46.98	20.90
Silty sand (%)	0	13.06	7.08
Mud (%)	15.31	47.25	28.27
Medium grain size (μm)	20.81	189.37	91.61
Sorting coefficient	1.68	6.32	2.67

Fig. 3 The compositions of Oligocene sandstone reservoirs in Lengdong area, Qaidam Basin. **a** Triangular diagram of main components of sandstone reservoirs. Three end members on the classification triangle chart fine-coarse sand, silty sand and mud. **b** Triangular diagram of sandstone classification. Three end members on the classification triangle chart are quart, feldspar and rock debris. **c** Lithological compositions triangular diagram. Three end members on the classification triangle chart are grains and pores, matrix and cements

Table 2 The compositions of Oligocene sandstone reservoirs in the Lengdong area

Detrital grains	Min	Max	Ave
Quartz (vol%)	37	57	47
Potassium feldspars (vol%)	1	5	3.21
Plagioclase feldspars (vol%)	5	13	8.08
Volcanic lithic fragments (vol%)	1	22	5.39
Metamorphic fragments (vol%)	6	26	17.17
Sedimentary fragments (vol%)	4	14	8.34
Mica (vol%)	1	6	3.39
Matrix (vol%)	1	25	5.54
Diagenetic alterations			
Calcite (vol%)	1	18	9
Dolomite (vol%)	0	22	2.3
Siderite (vol%)	0	2.4	1.1
Quartz overgrowth (vol%)	0	2.7	0.16
Clay minerals (vol%)	1	10	4.45
Illite (vol%)	30	77	53.8
Smectite (vol%)	3	13	7.35
Illite–smectite mixed layers (vol%)	4	64	22.92
Chlorite (vol%)	5	38	15.93
Porosity			
Intergranular porosity (vol%)	1	20	7.39
Intragranular porosity (vol%)	1	2	1.36

sandstone, pebbly sandstone, conglomeratic sandstone and conglomerate. Their sorting coefficients range from 1.68 (well-sorted) to 6.32 (poorly sorted). The sorting coefficient shows a positive relationship with the medium grain size.

The compositions of the Oligocene sandstone reservoirs in the Lengdong area are summarized in Table 2. Based on the statistical analyses of the cast thin sections, the sandstone classification of the interval of interest in the study area was performed using a triangular diagram (Folk et al.

1970) (Fig. 3b). The Lengdong sandstones are mainly feldspathic lithic sandstone, with an average composition of Q55.85F13.46R30.69. The analysis of lithological compositions indicates that the sandstones in the study area are dominated by pure sandstones and greywacke (Fig. 3c). The detrital feldspars include both potassium and plagioclase feldspar. The lithic fragments mainly comprise metamorphic fragments, followed by volcanic and sedimentary fragments. Mica represents 3.39% of the detrital components. The interstitial materials are dominated by carbonates, including calcite, dolomite and ankerite, with small amounts of quartz overgrowths and clay minerals (Table 2). The pores in the Lengdong area are dominated by intergranular pores (Table 2).

Porosity and permeability of the sandstone reservoir

The porosity and permeability values of the argillaceous sandstone, siltstone, fine sandstone, medium sandstone, conglomerate and conglomeratic sandstone are shown in Fig. 4. The fine sandstone has the widest distribution of porosity and permeability values. The silty sandstones have the smallest range of porosity and permeability values, while the maximum porosity and permeability values of the conglomeratic sandstone are much higher than those of the fine sandstone (Fig. 4). The porosity and permeability values of all sandstones show good linear relationships.

Oil saturation of the sandstone reservoir

The oil saturation conditions of different Oligocene sandstones in the Lengdong area are summarized in Fig. 5 (internal materials of CNPC). The conglomerate, fine sandstone and conglomeratic sandstone have the best oil saturation

Fig. 4 Cross plot of porosity and permeability of sandstone reservoirs from the Oligocene Xiaganchaigou Formation (E_3) in the Lengdong area, Qaidam Basin, China. Sandstone reservoirs include argillaceous sandstone, silty sandstone, fine sandstone, medium sandstone, pebbly sandstone, conglomeratic sandstone and conglomerate
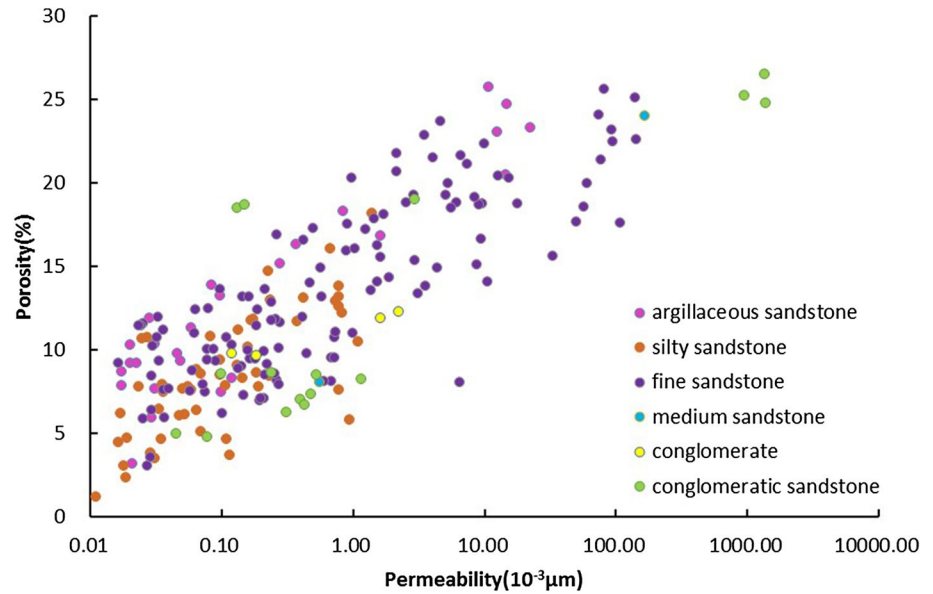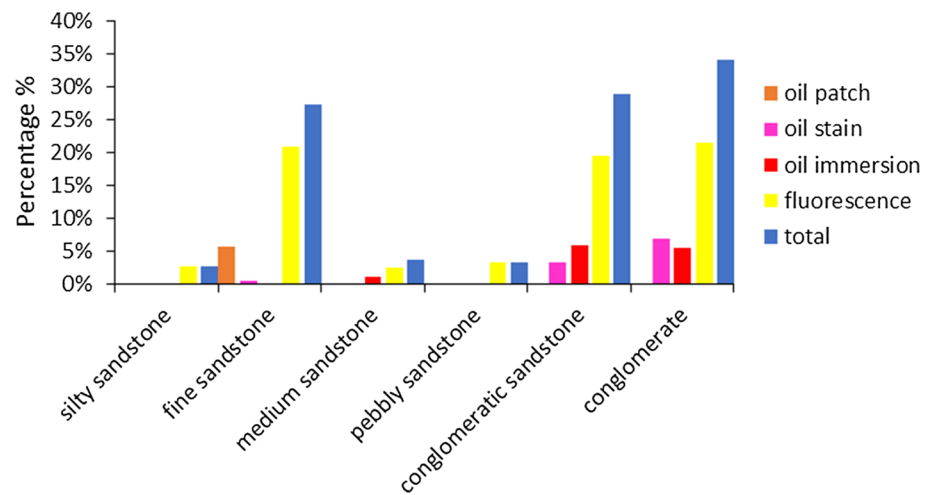

Fig. 5 Oil saturation values of argillaceous sandstone, silty sandstone, fine sandstone, medium sandstone, pebbly sandstone, conglomeratic sandstone and conglomerate reservoirs from the Oligocene Xiaganchaigou Formation (E_3) in the Lengdong area, Qaidam Basin

values, with high fluorescence contents. The oil stain and immersion values in conglomerate and conglomeratic sandstone reflect their relatively high contents, while in fine sandstone, the content of the oil patch is higher. The oil saturation values of silty sandstone, medium sandstone and pebbly sandstone are very limited, i.e., approximately 3%.

Sedimentological description

Based on abundant core observations and well logging, seismic and regional background data, we conclude that the sandstones of the Oligocene Xiaganchaigou

Formation (E_3) in the Lengdong area mainly represent a sandy braided river and braided delta system, with a limited area characterized by the development of an alluvial fan in the Lower Xiaganchaigou Formation (E_3^1) in the study area (Tang 2016) (Fig. 6). Five depositional facies are identified, consisting of distributary channel, interdistributary bay, mouth bar, central bar and distal sand sheet facies.
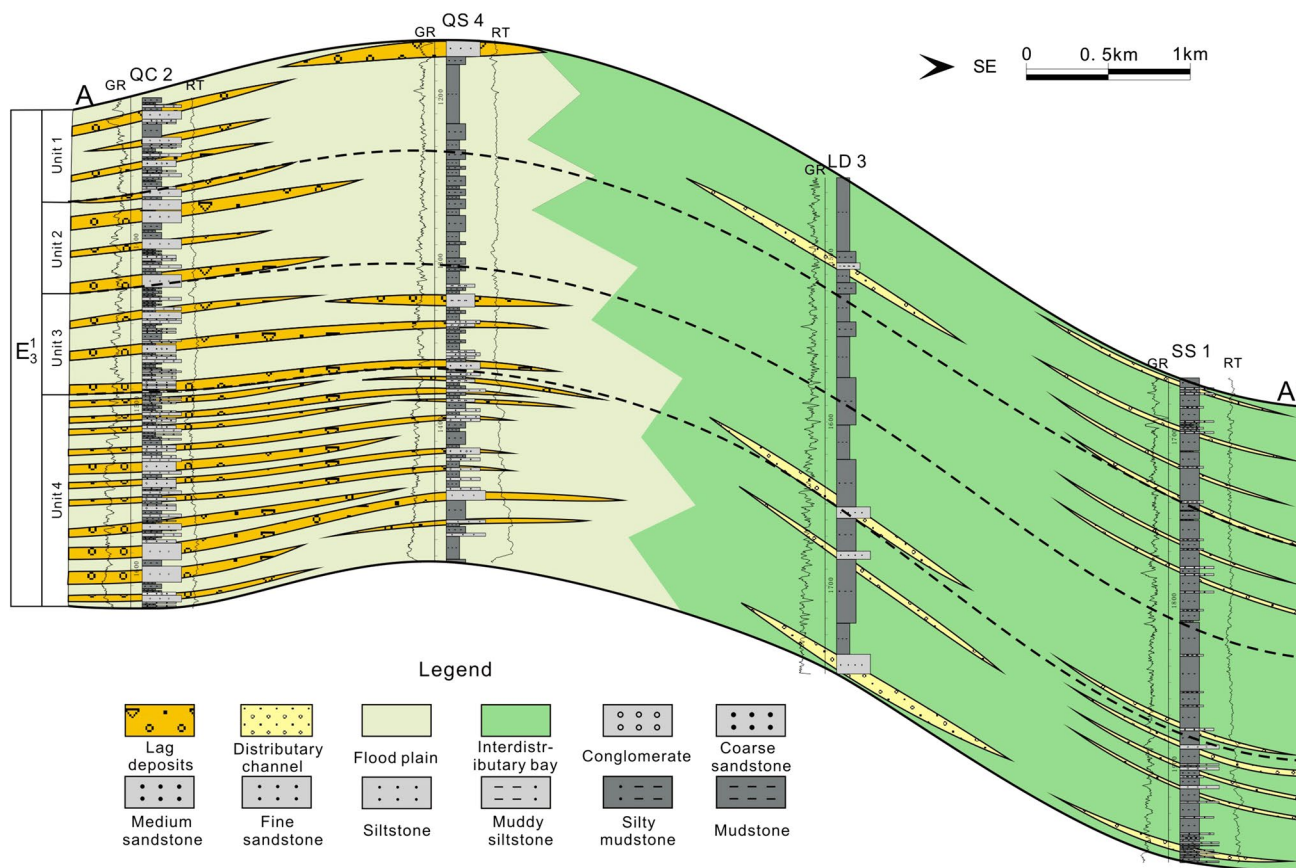
Fig. 6 Stratigraphic correlation section from well QC2 to well SS1 showing distribution of sedimentary facies in the Oligocene Lower Xiaganchigou Formation (E_3^1) in the Lengdong area, Qaidam Basin, China. The site of the section is marked in Fig. 2a

Log (GR)	Shape	Amplitude	Contact	Lithology	Description	Sedimentary facies
a Bell-shaped		Medium to high	Sharp erosional bottom contact, gradational top contact		well SX1,1461.4-1466m: Lithologies are pebbly sandstones, fine sandstones, pelitic siltstones and silty mudstones from bottom to top, with fining-upward sequence.	Middle alluvial fan braided river central bar braided delta plain
b Box-zigzag shaped		Medium to high	Both bottom and top are sharp		well LD3,641.9-647.9m: The grain size of the sediments is coarse. Sediments are dominated by conglomeratic sandstones interbedded with thin fine sandstones.	Middle alluvial fan braided river central bar braided delta plain Distributary channel
c Funnel-shaped		Medium to high	Gradational bottom contact, sharp erosional top contact		well QC1,814-818.8m: The lithologies are mudstones, silty mudstones and conglomeratic sandstones from bottom to top,with coarsening-upward sequence.	Mouth bar distal sand sheet outer alluvial fan
d Finger-shaped		Low to medium	Gradational contact at both the top and bottom		well QC1,1129-1134.9m: Sediments are dominated by conglomeratic sandstones. Sandstones are interbedded with mudstones.	Middle alluvial fan braided river floodplain

Fig. 7 Typical sedimentary log through the Oligocene Xiaganchaigou Formation (E_3) showing the distribution of major sedimentary facies and depositional environments. Characteristics, lithology and sedimentary facies of **a** Bell-shaped log. **b** Box-zigzag shaped log. **c** Funnel-shaped log. **d** Finger-shaped log

Distributary channel

The distributary channel facies is represented by superimposed fining-upward and thinning-upward channelized units of conglomerate, sandstone and mudstone (Fig. 7b). The coarser sandstones display planar and trough cross-stratification and massive bedding. The finer sandstones display low-angle cross and parallel stratification. Each unit has an erosional surface at its bottom marked by a lag deposit. The lag deposits usually consist of coarse conglomerate or pebbly sandstone. The grains of log deposits are moderately well-sorted and poorly to moderately rounded. Their well logs are box-shaped and characterized by sharp erosional bottom contacts and gradational top contacts. The distributary channel facies are interbedded with front bar or interdistributary bay facies (Fig. 6).

Interdistributary bay

This facies is normally located in the uppermost part of a bay-fill unit, and it consists of silts and silty clay. The typical sedimentary structures of the interdistributary bay facies are high bioturbation, silty and sandy stringers and scattered shell debris (Coleman 1981; Boggs 1995). The sandy deposits in this facies were probably formed by levee progradation or crevasse splay in an interdistributary lagoon (Amorosi and Marchi 1999). Their well logs are low-amplitude finger-shaped, with gradational contacts at both the bottom and top (Fig. 7d).

Mouth bar

The mouth bar facies is composed of siltstone and fine- to medium-grained sandstones. It is distributed marginal to or in front of the distributary channel facies and exhibits coarsening-upward cycles (Fig. 7c). In this facies, low-angular cross bedding, trough cross bedding, massive bedding, and current ripple and wave ripple lamination are usually developed. Its well logs are funnel-shaped, with gradational bottom contacts and sharp erosional top contacts.

Central bar

This facies consists of conglomerates (pebbly braided rivers) and sandstones (sandy braided rivers). Its grains exhibit moderate sorting and moderate rounding. The dominant structures of the central bar facies comprise parallel bedding, large-scale trough cross bedding and massive bedding. This facies displays a fining-upward vertical sequence (Fig. 7a). Its well logs are bell-shaped, with sharp erosional bottom contacts and gradational top contacts.

Distal sand sheet

This facies consists of thin, coarsening-upward sandstones interbedded with mudstones (Fig. 7c). The sandstones are fine- to very fine-grained, with wave ripple or parallel laminations. Compared to those of the mouth bar facies, the scales of the sedimentary structures in this facies are smaller, and the coarsening-upward sandstones are also finer-grained and thinner. The distal sand sheet facies is distributed in front of the distributary channel and is in close contact with the prodelta. Therefore, this facies is interpreted as a distal sand sheet facies (Galloway and Hobday 1983).
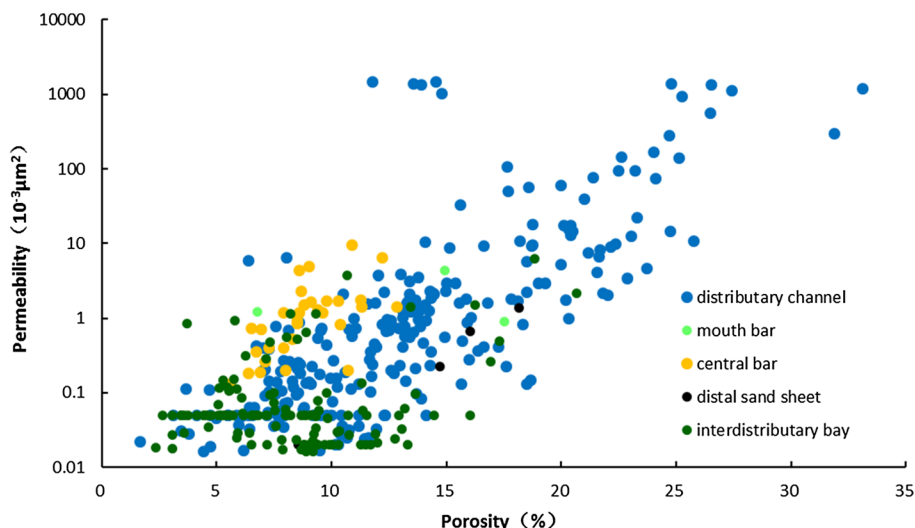
Porosity and permeability of sandstone

The sedimentary facies of the Oligocene Xiaganchaigou Formation (E_3) in the Lengdong area, Qaidam Basin, have some effects on the reservoir quality (Fuchtbauer 1983). The porosity and permeability values of the distributary channel sandstones range from 1.68 to 33.3% (av. 13.13%) and 0.02 to 1458.39×10^{-3} μm^2 (av. 62.05×10^{-3} μm^2), respectively. The porosity values of the sandstones in the mouth bar range from 1.68 to 33.3%, with an average value of 13.07%. The permeability values of the mouth bar sandstones range from 0.9×10^{-3} to 4.73×10^{-3} μm^2, with an average permeability value of 2.16×10^{-3} μm^2. The porosity and permeability values of the central bar sandstones range from 5.60 to 12.86% (av. 8.84%) and 0.13 to 9.40×10^{-3} μm^2 (av. 1.63×10^{-3} μm^2), respectively. The porosity values of the sandstones in the distal sand sheet range from 8.60 to 18.20%, with an average value of 14.40%. The permeability values of the distal sand sheet range from 0.02×10^{-3} to 1.38×10^{-3} μm^2, with an average permeability value of 0.57×10^{-3} μm^2. The reservoir quality is worst in the interdistributary bay, which has a porosity value of 7.67% and a permeability value of 0.13×10^{-3} μm^2 (Table 3). The sandstone reservoir in the distributary channel has the highest porosity and permeability values, followed by those in the

Table 3 Statistical table of relationship between physical parameters and microfacies in the Lengdong area

Microfacies types	Physical parameters $\left(\frac{\text{Min}-\text{Max}}{\text{Mean}}\right)$	
	Porosity (%)	Permeability (10^{-3} μm^2)
Distributary channel	1.68–33.3 / 13.13	0.02–1458.39 / 62.05
Mouth bar	6.77–17.54 / 13.07	0.90–4.37 / 2.16
Central bar	5.60–12.86 / 8.84	0.13–9.40 / 1.63
Distal sand sheet	8.60–18.2 / 14.40	0.02–1.38 / 0.57
Interdistributary bay	4.80–10.78 / 7.67	0.01–0.60 / 0.13

Fig. 8 Cross plots of porosity and permeability of sandstone reservoirs in distributary channel, mouth bar, central bar, distal sand sheet and interdistributary bay facies in the Oligocene Xiaganchaigou Formation (E₃) in the Lengdong area, Qaidam Basin

mouth bar and central bar. The sand sheet and interdistributary channel sandstone reservoirs have the lowest porosity and permeability values (Fig. 8).

Diagenesis

Compaction

Compaction is extensively developed in the Lengdong area. Based on petrographic analysis, line contacts, line-concavo-convex contacts and deformed ductile grains such as mica can be observed (Fig. 9a, b, c). The initial porosity values of the sandstone in the Lengdong area range from 27.40 to 31.09%, with an average value of 29.89%. The initial porosity values are calculated using the method presented by Beard and Weyl (1973).

$$Pprimary = 20.91 + (22.9/So) \tag{1}$$

$$\begin{aligned} Vcompaction = {} & Vprimary + Vdissolution \\ & - Vcementation - Vpresent \end{aligned} \tag{2}$$

$$Pcompaction = (Vcompaction/Vprimary) \times 100\% \tag{3}$$

where Pprimary is the primary porosity; So is the sorting coefficient; Vcompaction is the loss of pore volume due to compaction; Vprimary is the primary pore volume; Vdissolution is the increase in pore volume due to dissolution; Vcementation is the loss of pore volume due to cementation; Vpresent is the present pore volume; and Pcompaction is the percentage of porosity loss due to compaction.

The average loss of pore volume due to the compaction of the Xiagganchaigou (E₃) Formation in the Lengdong area, from bottom to top, is estimated to be 18.2%. The corresponding rate of porosity compaction loss is 48.6%.

With increasing depth, the porosity compaction loss rates increase. The compaction in the center of the sandstones shows line contacts and concavo-convex contacts, while in the vicinity of the sandstone–mud boundary, it mainly shows point contact.

Cementation

Cementation is one of the most important factors determining the reservoir quality in the study area. Carbonates, authigenic silicate minerals and clay minerals are the main cements in the study area (Zhang 2010). The content of carbonate cements is highest among the diagenetic alteration products, with an average value of 12.4%. Carbonate cements usually precipitate in the pores between particles and intragranular dissolution pores (Fig. 9d, e). The main carbonate cements in the study area are calcite (calcite and ferroan calcite) (av. 9%), dolomite (dolomite and ferroan dolomite) (av. 2.3%) and siderite (av. 1.2%). In some samples, calcite cement is dominant, and the pore spaces are completely blocked (Fig. 9f).

In this study, authigenic silicate minerals mainly refer to authigenic quartz. The authigenic quartz content ranges from 0 to 2.7% (av. 0.16%). Overgrowths of authigenic quartz usually occur on the edges of quartz in primary porosity (Fig. 9g). In a few cases, dust lines occur between two phases of quartz overgrowths (Fig. 9j). Another less widespread authigenic silicate mineral is represented by feldspar overgrowths. Authigenic feldspar forms in dissolution pores and is supported by illite (Fig. 9h).

The clay minerals mainly consist of matrix and authigenic clay minerals in sediments. XRD analysis reveals that the contents of clay minerals range from 8 to 51.2%, with an average value of 27.83%. SEM analysis reveals that the clay
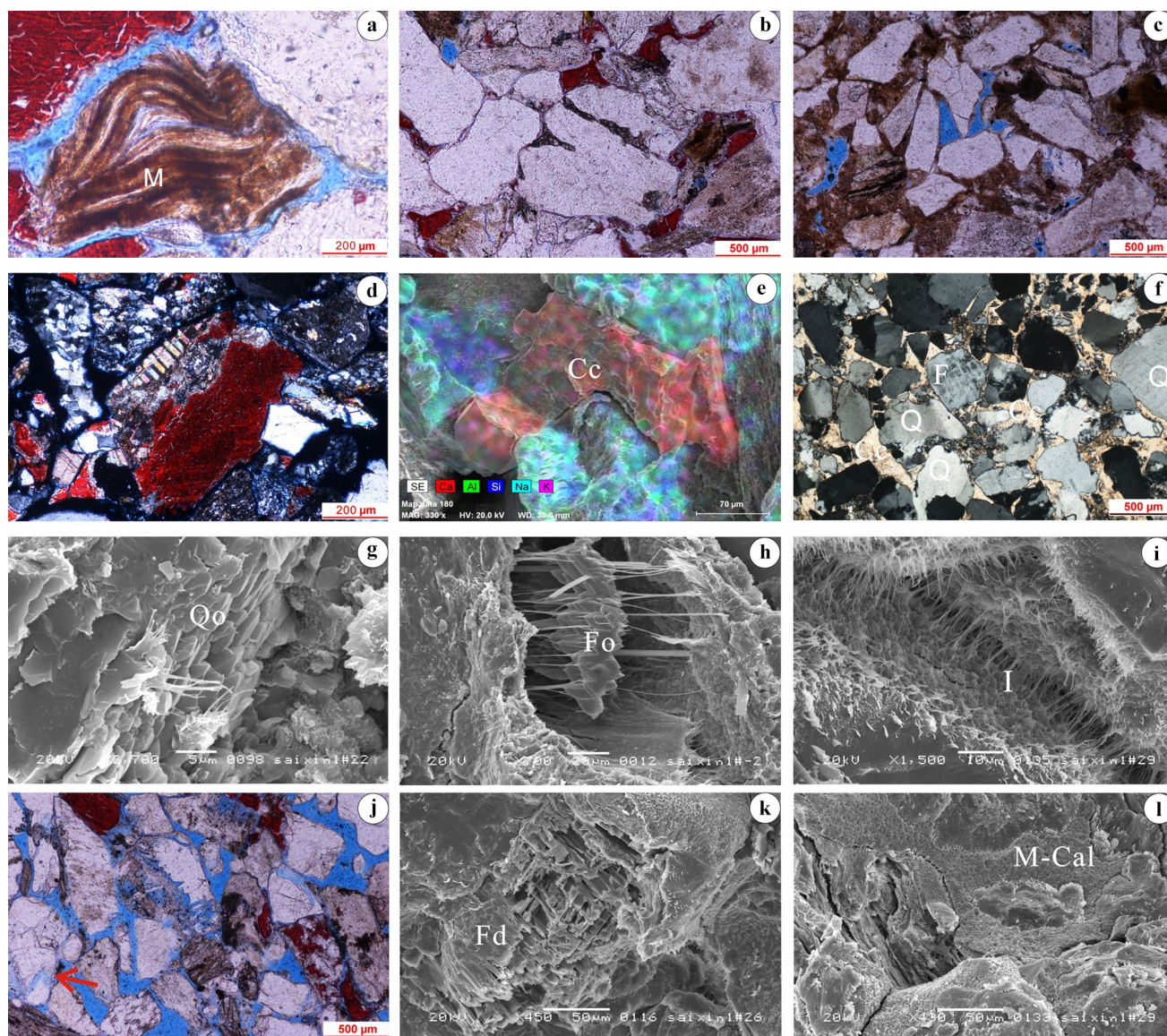
Fig. 9 **a** Optical photomicrograph of deformation of a mica as a result of compaction, well SX1, 1321.0 m (–). **b** Optical photomicrograph of line contacts and line-concavo-convex contacts of quartz, well SX1, 1310.50 m (–). **c** Optical photomicrograph showing point contacts and line contacts of quartz, well SX1, 1460.5 m (–). **d** Optical photomicrograph displaying carbonate cements precipitate in the pores among particles and intragranular dissolution pores, well SX1, 1310.5 m (–). **e** Energy spectrum analysis photomicrograph of well SX1, 1466.50 m, ×330. **f** Optical photomicrograph displaying calcite cements totally block the pore, Well Ld1, 1628 m (–). **g** SEM image of overgrowth of quartz, well SX1, 1454.00 m, ×2700.

h SEM image showing feldspar overgrowth supported by illite, well SX1, 1169.00 m, ×700. **i** The hair-like illites precipitate on the surface of minerals, well SX1, 1470.50 m, ×1500. **j** Optical photomicrograph displaying intergranular and intragranular pores generated by strong dissolution. Red arrow indicates the dust line between two phase quartz overgrowth well SX1, 1321.0 m (–). **k** SEM image showing dissolution of feldspar begins through cleavage, well SX1, 1466.50 m, ×450. **l** SEM image of poikilitic carbonate cement and micropores, well SX1, 3877.24 m, ×984. *Q* quartz, *F* feldspar, *M* mica, *I* illite, *Cc* calcite cement, *Qo* quartz overgrowth, *Fd* feldspar dissolution, *Fo* feldspar overgrowth, *M-Cal* microcrystalline calcite

minerals developing in the Lengdong area are almost all illite or illite/smectite. Illite and illite/smectite are mainly distributed on the surfaces of detrital particles or in the spaces between particles (Fig. 9i).

Compared to those of the authigenic quartz and clay minerals, the influence of carbonate cements on the

reservoir quality is very strong. In some samples, the intergranular pores are nearly completely occluded by calcite (Fig. 9f). In general, high contents of carbonate cements have negative effects on porosity and permeability. Specifically, the carbonate cements in the study area mainly consist of calcite cements. When the content of calcite
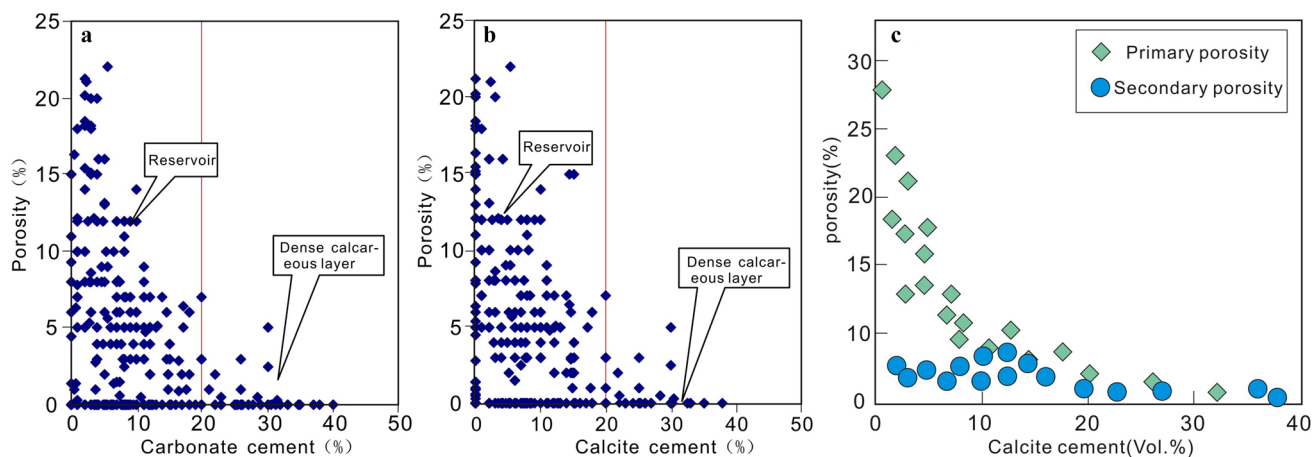
Fig. 10 **a** Cross plots of porosity and carbonate cement. **b** Cross plots of porosity and calcite cement. **c** Cross plots of primary and secondary porosity and calcite cement; primary porosity is indicated by green rhombus, and secondary porosity is indicated by blue circle. Porosity values of the Oligocene sandstone reservoirs are measured by the point counting of thin sections in the Lengdong area, Qaidam Basin

cement is greater than 20%, the sandstones will form a dense calcareous layer, and the effective reservoir thickness will become thinner. The porosity decreases sharply when the calcite cement content exceeds 20%. In the study area, sandstones with carbonate cement contents of 20% were identified as favorable reservoirs (Fig. 10a, b). As the calcite cement content increases, the primary intergranular pores decrease. The secondary pores increase when the calcite cement content is less than 20%; they then decrease rapidly when the calcite cement is greater than 20% (Fig. 10c).

The contents of carbonate rock in rock fragments range from 1 to 8%, with an average value of 3.5%. The loss in pore volume due to cementation can be calculated using Eq. (4).

$$Pcementation = (Vcementation/Vprimary) \times 100\% \qquad (4)$$

where Pcompaction is the percentage of porosity loss due to cementation.

The loss of pore volume due to cementation ranges from 1 to 25% (av. 7.6%), and the loss rate is 24.96%. These results indicate that carbonate cementation is another important factor influencing the reservoir quality in the Lengdong area.

Dissolution

The secondary pores of the Oligocene sandstone reservoirs in the Lengdong area are mainly formed by the dissolution of skeletal grains such as feldspar, calcite cements and matrix (Fig. 9j–l). Based on the analysis of thin sections, the increase in porosity caused by dissolution ranges from 2 to 15%, with an average value of 6.9%. In this study, we used the dissolution pore volume as the value of the pore volume

increased by dissolution (Vdissolution). The percentage of the porosity increased by dissolution (Pdissolution) is calculated using Eq. (5).

$$Pdissolution = (Vdissolution/Vprimary) \times 100\% \qquad (5)$$

where Pdissolution is the increase in pore volume due to dissolution. The dissolution of the Oligocene sandstone reservoirs in the Lengdong area is strong (Fig. 9j). The dissolution of feldspar tends to begin along its cleavage (Fig. 9k). The increase in secondary porosity caused by calcite cements is limited because it is compensated by the reprecipitation of calcite (Fig. 9i). The calcite cement contents, porosity values and pressure coefficients in the Upper Xiaganchaigou Formation (E_3^2) were analyzed from 1850 to 2166 m. The dissolution of calcite cements shows a negative relationship with the pressure coefficient, while the porosity shows a positive linear relationship with the pressure coefficient (Fig. 11a, b). Overpressure contributes to the secondary porosity of the Oligocene sandstone reservoirs in the Lengdong area.

Discussion

Diagenetic sequences

Based on thin section, paleotemperature, SEM, XRD and CL analyses, a schematic diagram of the diagenetic evolution of the sandstones in the Lengdong area is summarized in Fig. 12. Three major diagenetic evolution stages are recognized, including eodiagenesis A, eodiagenesis B and mesodiagenesis A. The Oligocene Xiaganchaigou Formation (E_3)
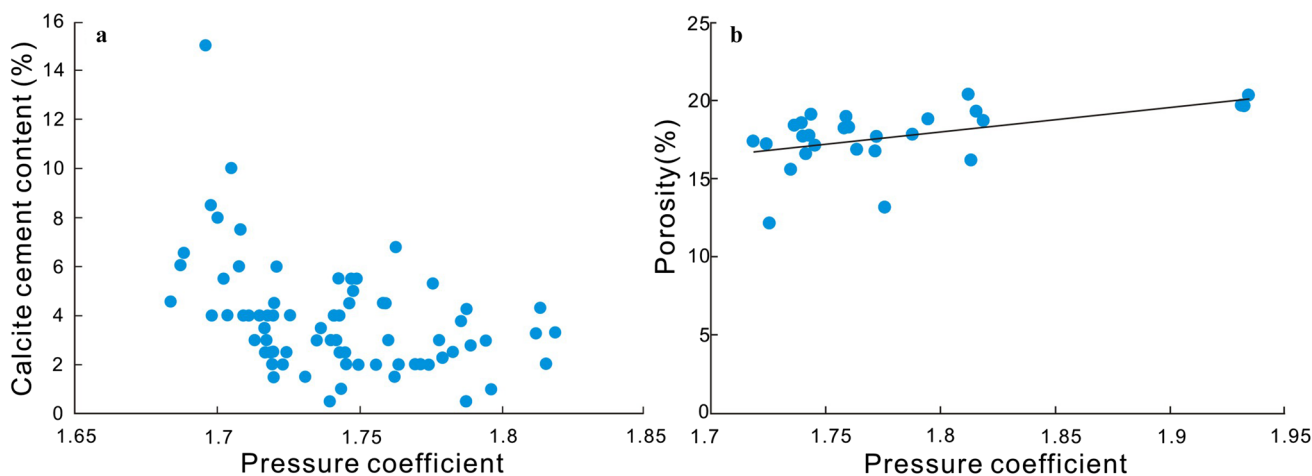
Fig. 11 **a** Cross plots of pressure coefficient and calcite cement content of sandstones in the Upper Xiaganchaigou Formation (E_3^2) in the Lengdong area, Qaidam Basin. **b** Cross plots of pressure coefficient and porosity of sandstones in the Upper Xiaganchaigou Formation (E_3^2) in the Lengdong Area, Qaidam Basin. Pressure coefficient refers to Tang (2016)

Fig. 12 The diagenetic sequence of sandstone reservoirs from the Oligocene Xiaganchaigou Formation (E_3) in the Lengdong area, Qaidam Basin
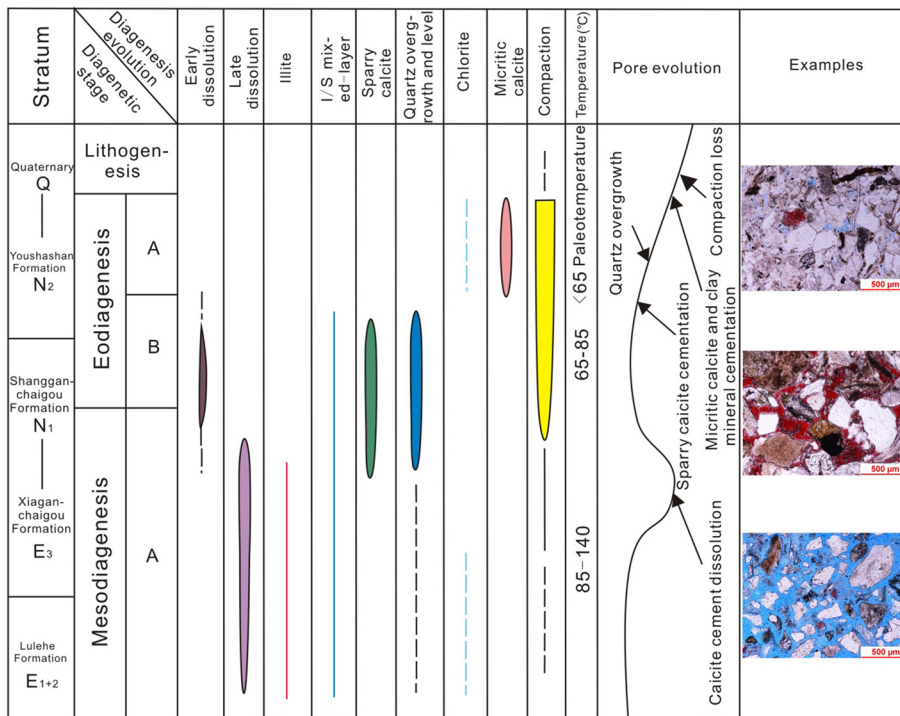
sandstones in the Lengdong area, Qaidam Basin, China, are in the eodiagenesis B and mesodiagenesis A stages.

In the eodiagenesis B stage, mechanical compaction was strengthened and the massive initial porosity decreased. As the burial depth increased, early calcite cements were dissolved, followed by the precipitation and grain replacement of late diagenetic calcite. Moreover, quartz replacement, quartz overgrowths and the formation of clay minerals (such as mixed-layer I/S) occurred. The temperature in the eodiagenesis B stage was less than 85 °C (Li et al. 2016).

During the mesodiagenesis A stage, the diagenetic minerals mainly included quartz, chlorite, illite, mixed-layer I/S, ferroan dolomite and feldspar. Ferroan dolomite formed during this stage. Illite and chlorite cements, as well as unstable grains such as feldspar, were significantly dissolved. A large amount of secondary porosity

developed. The temperatures in this stage ranged from 85 to 140 °C (Li et al. 2016).

Effects of sedimentary facies on reservoir quality

The sedimentary facies has a significant effect on the composition and texture of sandstone; thus, it can influence subsequent diagenesis and affect the reservoir quality.

The clastic particles in the distributary channel, mouth bar and central bar, where the hydrodynamic force is strong, have the characteristics of coarser grains, low matrix contents, well-sorted textures and high degrees of compositional maturation. Due to their high quartz contents and low debris contents, their reservoirs are better able to resist compaction. The sandstones in the distributary channel, mouth bar and central bar had large amounts of initial porosity and permeability. They experienced weak compaction; thus, their initial porosity was preserved. Primary porosity can be a good conduit for the migration and storage of pore fluid, thus forming second porosity due to dissolution. However, the sandstones in the interdistributary bay and distal sand sheet facies were deposited in a low-energy environment with fine-grained and clay-rich sediment. They were poorly sorted, with high matrix contents. Cementation tends to occur in reservoirs that form in such low-energy environments. As the porosity and permeability of these sandstones are very low, their reservoirs are tight.

Diagenetic controls on reservoir quality

The reservoir quality of sandstone is strongly influenced by diagenesis. Based on the calculation of Pcompaction, Pcementation and Pdissolution, the average losses of pore volume due to compaction and cementation are 48.62% and 24.96%, respectively. The average increase in porosity due to dissolution is 6.9%. We can conclude that compaction, cementation and dissolution have large effects on the reservoir quality of the Oligocene sandstone in the Lengdong area, Qaidam Basin.

Compaction is intensively developed in the lithogenesis stage, when sediments are unconsolidated. These sediments are then consolidated and dehydrated with increasing pressure. With increasing burial depth, the porosity of sandstone generally decreases because of the effects of compaction. In the early diagenesis stage, the high contents of mechanically unstable compositions lead to rapid decrease in porosity and permeability during burial due to the influence of mechanical compaction. Ductile compaction occurs when some detrital grains, such as micas and lithic fragments, undergo both intergranular rearrangements and plastic deformation. The changes in grain contacts greatly reduce the primary intergranular porosity. The deformed flakes of micas may

locally prevent fluid migration. Plastic deformation tends to cause ductile grains to smear around harder grains, such as quartz, thus efficiently reducing porosity during burial. The ductile deformation occurring during this detrital compaction leads to the increasing stress sensitivity in sandstone. When a reservoir has high contents of rigid grains (i.e., quartz) and carbonate cements, compaction can be limited (Lima and De Ros 2002).

The main cements in the Lengdong area are carbonate cements, authigenic silicate minerals and clay minerals. Among these, carbonate cements are the most significant diagenetic minerals. Calcite is the dominant carbonate cement in the Lengdong area, while dolomite and siderite cements are randomly distributed; external and internal sources are believed to contribute to the carbonate cements in clastic reservoirs (Dutton 2008). The most common internal sources of carbonate cement are the thermal evolution of kerogen in mudstone (Dutton 2008), the diagenesis of interbedded mudstones (Milliken and Land 1993; Li et al. 2014), the dissolution of K-feldspar and conversion of kaolinite to illite in mudstones, as well as the conversion of smectite to illite (Li et al. 2014). The chemical materials generated by alteration in mudstones can be transferred to sandstones by diffusion with a chemical gradient. Then, the chemical equilibrium in a sandstone will be broken, and carbonate cements will precipitate. The dissolution of carbonate skeletal grains may also provide a source for carbonate cementation (Carvalho et al. 1995). Calcite cements mainly fill in intergranular pores and the intragranular dissolved pores of detrital grains, such as those caused by feldspar dissolution. The losses of porosity and permeability due to calcite cements are greater than those due to coating cement (i.e., clay minerals and quartz overgrowths). A calcite cement volume of higher than 20% is regarded as a dense calcareous layer because fluid will have difficulty migrating through it. When the calcite cement is less than 20%, the secondary porosity increases slightly. Calcite cements have many potential sources, including the dissolution of detrital carbonate rock fragments, the diagenesis of interbedded mudstones, the dissolution of K-feldspar, the conversion of kaolinite to illite in mudstones and the conversion of smectite to illite. The sandstone in the Lengdong area contains relatively high contents of muddy clasts. Petrographic data indicate that high calcite cement volumes tend to be distributed in the mudstone–sandstone contact boundaries. Therefore, the major source of calcite cements in the study area is interpreted to be derived from external mudstones and internal muddy clasts. The CO_3^{2-} ions may be derived from kerogen maturation, as there are several oils in the Lengdong area (Dutton 2008) (Fig. 2b). The necessary ion components, such as Fe^{2+}, Mg^{2+} and Ca^{2+}, may be derived from the conversion of smectite to illite (Narkiewicz et al. 1982), the dissolution of K-feldspar and the associated illitization of

kaolinite (Macaulay et al. 1993). Then, the mass transfer by fluid allows for the precipitation of calcite cements in sandstone.

The dissolution of unstable detrital grains such as feldspars and rock fragments is commonly observed in the study area (Fig. 9k). The dissolution of potassium, plagioclase feldspar and rock fragments increases with depth. At greater depths, the main secondary pores are produced by the dissolution of detrital grains and calcite cements. The dissolution of unstable silicate grains and the formation of abundant secondary porosity require the interaction of the sandstone with acidic fluids (Wilkinson et al. 2001). This acidic fluid may be derived from meteoric water (Mansurbeg et al. 2012) or pore water containing CO_2 released from maturing kerogen and organic acids (Crossey et al. 1984; Morad et al. 2000). During the Oligocene, the continuous uplift of the Altun Mountains led to the denudation of the Lengdong area (Xiao et al. 2005). The cracks that formed during uplift provided favorable conduits for the downward penetration of meteoric freshwater from the Earth's surface to these sandstone beds. The meteoric freshwater leaching of feldspars, calcite minerals and unstable detrital grains enhanced secondary porosity due to dissolution. In addition, several sets of hydrocarbon source rocks have been developed in the Lengdong area (Men et al. 2001). In the middle and late diagenesis stages, organic matter quickly decomposed and then produced acidic fluid under high-temperature and -pressure conditions, resulting in an acidic medium of pore water during the process of sedimentation (Crossey et al. 1986). This acidic fluid intensively dissolved the unstable components in these rocks, such as feldspar and debris. The temperatures required for this massive dissolution are 85 to 140 °C, which are similar to the concentrations of organic acid anions (Crossey et al. 1984). Therefore, the possible interpretation of dissolution in the mesodiagenesis stage in the Oligocene Xiaganchaigou Formation (E_3) of the Lengdong area is related to meteoric water during the late Oligocene and middle Miocene uplift and the addition of CO_2 and organic acids during the thermal maturation of hydrocarbon organic matter in the source rocks. Another contributor to the dissolution in the study area is overpressure. Overpressure can preserve some pores; however, it can also enable acidic fluid to migrate into sandstones and dissolve their calcite cements.

Classifications of reservoirs

The above discussion indicates that the reservoir quality of the sandstones from the Oligocene Xiaganchaigou Formation (E_3) in the Lengdong area, Qaidam Basin, China, is mainly controlled by their sedimentology, petrography and diagenesis. The diagenesis in the study area is mainly due to compaction, cementation and dissolution.

Table 4 The classification standard of influence extent on reservoir quality of compaction, cementation and dissolution of Oligocene sandstone reservoirs in the Lengdong area

Intensity	Pcompaction (%)	Pcementation (%)	Pdissolution (%)
Strong	> 70	> 70	> 70
Medium	70–30	70–30	70–30
Weak	30–0	30–0	30–0

To evaluate the reservoir quality of the sandstones from the Oligocene Xiaganchaigou Formation (E_3) in the Lengdong area, Qaidam Basin, China, the sandstone compositions, diagenesis (compaction, cementation and dissolution) and sedimentary facies are selected to comprehensively evaluate their weights based on their effects on reservoir quality (Table 5). The total evaluating parameter is assumed to be 1, and it is divided into five equal parts of 0.2. The good, moderate and bad reservoirs are given evaluating weights of 1, 0.7 and 0.4, respectively. The total evaluation score is the result of multiplying all five controlling factors by 0.2 and adding them. To indicate the diagenetic intensity of compaction, cementation and dissolution, a classification standard in the study area is defined by Pcompaction, Pcementation and Pdissolution (Wang et al. 2017) (Table 4). When the Pcompaction, Pcementation and Pdissolution value of a reservoir is greater than 70%, we define it as "Strong". When this value falls between 30 and 70%, the intensity of compaction, cementation and dissolution is medium. "Weak" intensity indicates a Pcompaction, Pcementation and Pdissolution value falling between 0 and 30%.

The comprehensive evaluation scores of the Oligocene sandstone reservoirs in the Lengdong area are classified based on Table 5. They are evaluated as (1) good: the best reservoir type. Good reservoirs mainly develop in distributary channels, and their compositions are fine sandstone, conglomerate and conglomeratic sandstone. Good reservoirs underwent weak compaction, weak cementation and strong dissolution, with calcite cement contents of less than 20%; (2) moderate: the reservoir quality is moderate. These reservoirs mainly include medium sandstone and silty sandstone in distal sand sheet, mouth bar and central bar sedimentary facies with medium compaction, cementation and dissolution; and (3) bad: the porosity and permeability values of bad reservoirs are the lowest. These reservoirs comprise argillaceous sandstone and pebbly sandstone with strong compaction, strong cementation (calcite cement contents of more than 20%) and weak dissolution in interdistributary bay facies.

Based on their total evaluation scores, the classification standards of the reservoir types of the Oligocene sandstone reservoirs in the Lengdong area are shown in Table 6. The total evaluating scores of 0.8–1 are defined

Table 5 Comprehensive evaluating of reservoir type classifications of Oligocene sandstone reservoirs in the Lengdong area

Evaluation	Good [1]	Moderate [0.7]	Bad [0.4]
Sandstone compositions (0.2)	Fine sandstone, conglomerate, conglomeratic sandstone	Medium sandstone, silty sandstone	Argillaceous sandstone, pebbly sandstone
Compaction (0.2)	Weak	Medium	Strong
Cementation (0.2)	Weak (cc < 20%)	Medium	Strong (cc > 20%)
Dissolution (0.2)	Strong	Medium	Weak
Sedimentary facies (0.2)	Distributary channel	Distal sand sheet, mouth bar, central bar	Interdistributary bay

Cc calcite cement content, the numbers in '()' stands for evaluating parameters and '[]'stands for evaluating weights

Table 6 The classification standard of reservoir types of Oligocene sandstone reservoirs in the Lengdong area

| Types	Type A	Type B	Type C
Total score	0.8	0.8–0.6	< 0.6

as type A, and those of 0.6–0.8 are classified as type B. The total evaluating sore of type C is less than 0.6. Type A sandstone is evaluated as the best reservoir, and type B sandstone is a moderate reservoir, while type C sandstone has the worst reservoir quality. The distribution of the reservoir type of Oligocene sandstone reservoirs in the Lengdong area is shown in Fig. 13. Type A sandstone reservoirs are mainly distributed in the center of the Lengdong area, showing a hook shape. These are favorable reservoirs for hydrocarbon exploration. Type B sandstone reservoirs are located at the edge of and inside type A reservoirs. Type C sandstone reservoirs are located at the outer edge of the study area. Type C is the last target to consider when looking for a good reservoir.

Conclusions

1. Two diagenetic evolution stages were recognized in the Oligocene Xiaganchaigou Formation (E_3) in the Lengdong area, Qaidam Basin: (1) during eodiagenesis stage B, mechanical compaction strengthened, quartz overgrowths formed and early calcite cement was dissolved; and (2) during mesodiagenesis stage A, illite and chlo-

Fig. 13 The distribution of sandstone reservoir types of the Oligocene Xiaganchaigou Formation (E_3) in the Lengdong area, Qaidam Basin
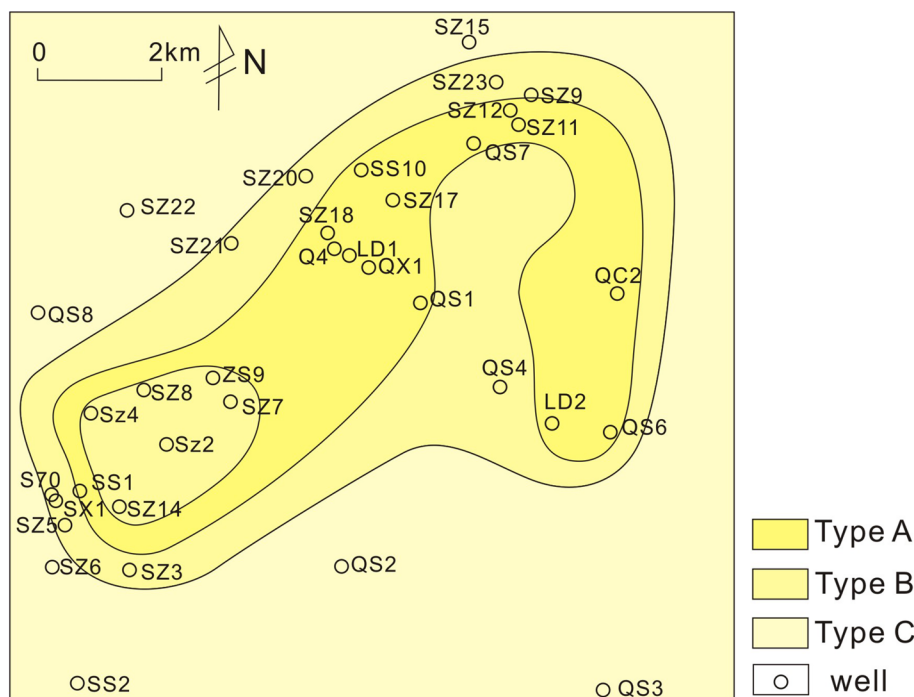
rite cements were significantly dissolved and massive secondary porosity formed.

2. Sedimentary facies control the reservoir quality by affecting the composition and texture of the sandstones. The sandstones in the distributary channel, mouth bar and central bar facies are well-sorted, with low matrix contents and high quartz contents. Compaction in these facies is relatively weak. They maintain their high initial porosity and permeability values. In contrast, the sandstone reservoirs in the interdistributary bay and distal sand sheet facies have high contents of matrix and ductile minerals. They are intensively compacted, and these reservoirs are dense.

3. The main diagenesis in the study area is compaction, cementation and dissolution. Compaction significantly reduces the initial porosity. The carbonate cement has a dominant influence on the reservoir quality. Dissolution increases the secondary porosity by dissolving the unstable detrital grains and calcite cements.

4. Based on the comprehensive analysis of their petrography, diagenesis and sedimentary facies, the sandstone reservoirs from the Oligocene Xiaganchaigou Formation (E_3) in the Lengdong area are classified into three types of good to bad exploration targets: type A, type B and type C. The classification of these reservoir types will contribute to further studies in similar areas.

References

Amorosi A, Marchi N (1999) High-resolution sequence stratigraphy from piezocone tests: an example from the Late Quaternary deposits of the southeastern Po Plain. Sed Geol 128:67–81

Beard DC, Weyl PK (1973) Influence of texture on porosity and permeability of unconsolidated sand. AAPG Bull 57(2):349–369

Boggs S (1995) Principles of sedimentology and stratigraphy. Prentice Hall, Upper Saddle River, pp 355–376

Cao ZL, Sun XJ, Wang LQ, Yan CF, Zhao J, Ma F (2013) The gas accumulation conditions of Dongping-Niudong slope area in front of Aerjin Mountain of Qaidam Basin. Nat Gas Geosci 24:1125–1131 **(in Chinese with English abstract)**

Carvalho MVF, De Ros LF, Gomes NS (1995) Carbonate cementation patterns and diagenetic reservoir facies in the Campos Basin Cretaceous turbidites, offshore eastern Brazil. Mar Pet Geol 12(7):741–758

Chen B, Chen FJ, Wu ZX, Zhou F, Sun GQ, Shi JA (2015) Diagenesis and favorable diagenetic facies of Paleogene Lulehe Formation sandstone in Lenghu region. Geol Sci Technol Inf 34(4):20–27 **(in Chinese with English abstract)**

Coleman JM (1981) Deltas: processes of deposition and models for exploration. International Human Resources Development Corp, Boston, p 91

Crossey LJ, Frost BR, Surdam RC (1984) Secondary porosity in laumontite-bearing sandstones: part 2. Aspects of porosity modification. AAPG Bull 59:225–237

Crossey LJ, Surdam RC, Lahann R (1986) Application of organic/inorganic diagenesis to porosity prediction. Roles Org Matter Sediment Diagenesis 147–155

Dickinson WR (1970) Interpreting detrital modal of graywacke and arkose. J Sediment Petrol 40:695–707

Dutton SP (2008) Calcite cement in Permian deep-water sandstones, Delaware Basin west Texas: origin, distribution, and effect on reservoir properties. AAPG Bull 92(6):765–787

Folk RL, Peter B, Andrew S, Lewis DW (1970) Detrital sedimentary rock classification and nomenclature for use in New Zealand. N Zeal J Geol Geophys 13(4):937–968

Fu ST, Ma DD, Guo ZY, Feng C (2015) Strike-slip superimposed Qaidam Basin and its control on oil and gas accumulation, NW China. Pet Explor Dev 42(6):778–789

Fuchtbauer H (1983) Facies controls on sandstone diagenesis. In: Sediment diagenesis. Springer, Dordrecht 269–288

Galloway WE, Hobday DK (1983) Terrigenous clastic depositional systems: applications to fossil fuel and ground water resources. Springer, Berlin, pp 81–113

Hillier MS, Hillier FS (2001) Conventional optimization techniques. In: Computational combinatorial optimization. Springer, Berlin, Heidelberg, pp 561–567

Jia YY, Shi JA, Shen YS, Zhou F, Sun GQ (2013) Research of structural reservoir in no.5 unit of Lenghu area. J Southwest Pet Univ (Nat Sci Ed) 35(4):43–50 **(in Chinese with English abstract)**

Jing B, Wang YD, Song C, Feng Y, Hu CH, Zhong SR, Yang JW (2017) Cenozoic sediment flux in the Qaidam Basin, northern Tibetan plateau, and implications with regional tectonics and climate. Glob Planet Chang 155

Jolivet M, Brunel M, Seward D, Xu Z, Yang J, Roger F, Tapponnier P, Malavieille J, Arnaud N, Wu C (2001) Mesozoic and Cenozoic tectonics of the northern edge of the Tibetan plateau: fission-track constraints. Tectonophysics 343(1–2):111–134

Li FJ, Meng LN, Fang CG, Li L, Lin H (2012) Palaeogeographic evolution of the Paleogene and Neogene in north margin of Qaidam Basin. J Palaeogeogr 14(5):596–606 **(in Chinese with English abstract)**

Li Q, Jiang Z, Liu K, Zhang C, You X (2014) Factors controlling reservoir properties and hydrocarbon accumulation of lacustrine deep-water turbidites in the Huimin depression, Bohai Bay Basin, east China. Mar Pet Geol 57(2):327–344

Li ZX, Gao J, Li WF, Wu JF, Liu CL, Ma YS (2016) The characteristics of geothermal field and controlling factors in Qaidam Basin, Northwest China. Earth Sci Front 23(5):023–032 **(in Chinese with English abstract)**

Lima RD, De Ros LF (2002) The role of depositional setting and diagenesis on the reservoir quality of Devonian sandstones

from the Solimoes Basin, Brazilian Amazonia. Mar Pet Geol 19(9):1047–1071

Luo XR, Ying S, Wang LQ, Xiao AC, Ma LX, Zhang XB, Wang ZM, Song CP (2013) Dynamics of hydrocarbon accumulation in the west section of the northern margin of the Qaidam Basin, NW China. Pet Explor Dev 40(2):170–182

Macaulay CI, Haseldine RS, Fallick AE (1993) Distribution, chemistry, isotopic composition and origin of diagenetic carbonates: Magnus Sandstone, North Sea. J Sediment Res 63(1):33–43

Mansurbeg H, Ros LFD, Morad S, Ketzer JM, El-Ghali MAK, Caja MA, Othman R (2012) Meteoric-water diagenesis in late Cretaceous canyou-fill turbidite reservoirs from the Espirito Santo Basin, eastern Brazil. Mar Pet Geol 37(1):7–26

Men XY, Zhao WZ, Yu HL (2001) Oil and gas reservoir conditions and exploration proposal from Lenghu area in northern Qaidam Basin. Pet Explor Dev 28(4):4–7 (in Chinese with English abstract)

Milliken KL, Land LS (1993) The origin and fate of silt sized carbonate in subsurface Miocene–Oligocene mudstones, south Texas Gulf Coast. Sedimentology 40(1):107–124

Moore DM, Reynolds RCJ (1989) Identification of clay minerals and associated minerals. In: X-ray Diffraction and the Identification and Analysis of Clay Minerals. Oxford University Press, Oxford

Morad S, Ketzer JM, De Ros LF (2000) Spatial and temporal distribution of diagenetic alterations in siliciclastic rocks: implications for mass transfer in sedimentary basins. Sedimentology 47(Supplement s1):95–120

Narkiewicz M, Price RC, Mchargue TR (1982) Dolomite from clay in argillaceous or shale-associated marine carbonates; discussion and reply. J Sediment Res 52(3):873–886

Pang XQ, Zhou XY, Jiang ZX, Wang ZM, Li SM, Tian J (2012) Hydrocarbon reservoirs formation, evolution, prediction and evaluation in the superimposed basins. Acta Geol Sin 86(1):1–103

Ritts BD, Hanson AD, Zinniker D, Moldowan JM (1999) Lower-Middle Jurassic nonmarine source rocks and petroleum systems of the northern Qaidam Basin, northwest China. AAPG Bull 83(12):1980–2005

Tang JR (2016) Sealing capacity of tertiary caprock in Lenghu structural belt, northern margin of Qaidam Basin. Dissertation, China University of Geosciences (in Chinese with English abstract)

Tian GR, Yan C, Tuo JC, Wang P (2011) Late hydrocarbon accumulation characteristic of coal related gas in northern Qaidam basin. Nat Gas Geosci 22(6):1028–1032 (in Chinese with English abstract)

Tian JX, Li J, Pan CF, Tan Z, Zeng X, Guo ZQ, Wang B, Zhou F (2018) Geochemical charateristics anf factors controlling natural gas accumulation in the northern margin of the Qaidam Basin. J Pet Sci Eng 160:219–228 (in Chinese with English abstract)

Van Der Plas L, Tobi AC (1965) A chart for judging the reliability of point counting results. Am J Sci 263:87–90

Wang J, Cao YC, Liu KY, Liu J, Muhammad K (2017) Identification of sedimentary-diagenetic facies and reservoir porosity and permeability prediction: an example from the Eocene beach-bar sandstone in the Dongying depression, China. Mar Pet Geol 82:69–84

Wilkinson M, Milliken KL, Haszeldine RS (2001) Systematic destruction of K-feldspars in deeply buried rift and passive margin sandstones. J Geol Soc 158(4):675–683

Xiao AC, Chen ZY, Yang SF, Ma LX, Gong QL, Chen YZ (2005) The study of late Cretaceous paleostructural characteristics in northern Qaidam Basin. Earth Sci Front 12(4):451–457 (in Chinese with English abstract)

Yin A, Dang YQ, Zhang M, Chen XH, Mcrivette MW (2008) Cenozoic tectonic evolution of the Qaidam Basin and its surrounding regions (part 3): structural geology, sedimentation, and regional tectonic reconstruction. Geol Soc Am Bull 120(7):847–876

Zhang Y (2010) The diagenesis research on the west part of the Northern margin in the Qaidam Basin. Dissertation, Chengdu Universitty of Technology (in Chinese with English abstract)

Zhao R, Chen S, Wang H. Yan DT, Cao HY, Gong Y, He J, Wu ZX (2018) Paleogene sedimentation changes in Lenghu area, Qaidam Basin in response to the India–Eurasia collision. Int J Earth Sci (Geol Rundsch). https://doi.org/10.1007/s00531-018-1640-8

Zuffa GC (1980) Hybrid arenites: their composition and classification. J Sediment Pet 50:21–30

Affiliations

Jie He[1,2] · Hua Wang[1,2] · Chengcheng Zhang[4] · Xiangrong Yang[1,2] · Yunfei Shangguan[1,2] · Rui Zhao[1,2] · Yin Gong[1,2] · Zhixiong Wu[3]

[1] Key Laboratory of Tectonics and Petroleum Resources, China University of Geosciences, Wuhan 430074, China

[2] Faculty of Earth Resources, China University of Geosciences, Wuhan 430074, China

[3] Research Institute of Exploration and Development, PetroChina Qinghai Oilfield Company, Dunhuang 736202, China

[4] Nanjing Center of Geological Survey, China Geological Survey, Nanjing 210016, China